An investigation of macro- and micro-structural properties of concrete with ceramic waste powder as a sustainable cement substitute

Journal of Building Engineering 116 (2025) 114634

Contents lists available at ScienceDirect

Journal of Building Engineering

journal homepage: www.elsevier.com/locate/jobe

An investigation of macro- and micro-structural properties of concrete with ceramic waste powder as a sustainable cement substitute

Le Li [a], Boran Zhang [b], Paul Joseph [a], Xuelin Zhang [a], Lihai Zhang [b,*]

[a] Institute for Sustainable Industries & Liveable Cities (ISILC), Victoria University, 70-100 Ballarat Rd, Footscray, VIC, 3011, Australia
[b] Department of Infrastructure Engineering, The University of Melbourne, Grattan Street, Victoria, Parkville, VIC, 3010, Australia

ARTICLE INFO

Keywords:
Ceramic waste powder
Strength development
Thermal insulation
Porosity
Pozzolanic reaction

ABSTRACT

Previous studies have demonstrated that replacing cement with Ceramic Waste Powder (CWP) in concrete production is feasible without compromising the fundamental properties of the concrete. However, there is limited understanding of how CWP affects the development of strength during curing, as well as the thermal insulation performance at both ambient and elevated temperatures. Gaining insights into these property changes is essential to support the broader adoption of CWP in concrete applications. Moreover, few studies have quantitatively assessed the impact of CWP on the microstructural properties of concrete, including porosity, the extent of pozzolanic and alkali-silica reactions (ASR), and the degree of cement hydration. Understanding these micro-level changes is crucial for elucidating the mechanisms underlying improvements in strength, durability, and thermal performance, when cement is partially replaced by CWP. To address these gaps, this paper presents a comprehensive experimental investigation of the macro- and micro-properties of concrete with 10 % and 20 % cement replaced by CWP. The results show that replacing up to 20 % of cement with CWP enhances early-age strength development and thermal insulation compared to conventional concrete. Additionally, a 20 % CWP replacement reduces porosity, increases pozzolanic activity and cement hydration, and does not significantly trigger ASR. This study also compares CWP with other commonly used supplementary cementitious materials (SCMs), such as silica fume, fly ash and slag. The comparison indicates that CWP can improve both macro- and micro-properties by reducing porosity and enhancing pozzolanic activity, performing comparably to, or better than, conventional SCMs.

1. Introduction

Concrete is the main material used in building and infrastructure construction, with an annual consumption of 30 billion tons. The increasing demand for cement in concrete manufacturing has led to serious environmental concerns. The latest International Energy Agency report indicated that global carbon dioxide (CO_2) emissions exceeded 33 gigatons in 2019 [1], of which cement production accounted for 5–7 % of the global anthropogenic emissions [2]. Cement production has other negative environmental impacts, such as water and noise pollution. Therefore, improving concrete sustainability and replacing cement with other materials is essential.

Ceramic waste powder (CWP) generated by the cutting and polishing of ceramic products (e.g., ceramic tiles) demonstrated

* Corresponding author.
E-mail address: lihzhang@unimelb.edu.au (L. Zhang).

https://doi.org/10.1016/j.jobe.2025.114634
Received 18 June 2025; Received in revised form 2 November 2025; Accepted 10 November 2025
Available online 12 November 2025

potential as Supplementary Cementitious Materials (SCMs) in concrete manufacturing. Li, Joseph, Zhang and Zhang [3] tested the engineering properties of concrete when CWP replaced 10 %–20 % of cement, and the results indicated that using up to 20 % of CWP to replace cement in concrete manufacturing is feasible without compromising the strength of the finished products. In this context, the compressive strength increased by 8.75 % when CWP replaced 10 % of cement. Also, this study found that replacing cement with 20 % CWP can improve the concrete's thermal insulation and fire performance (less mass loss and less mechanical property degradation after fire exposure). Bhargav and Kansal [4], Gautam, Kalla, Jain, Choudhary and Jain [5], and Parashar, Sharma and Sharma [6] also indicated that there is an improvement in concrete strength when CWP replaced cement. Conflict findings were reported by Kannan, Aboubakr, El-Dieb and Taha [7], Raval, Patel and Pitroda [8] and Patel, Arora and Vaniya [9] on the changes in concrete strength when CWP replaced cement. These studies indicated a reduction in compressive strength when 10 %–20 % CWP replaced cement. Nonetheless, these reductions are within the acceptance tolerance (±15 %) according to IS456 [10]. Thus, previous research consistently states that using 20 % CWP to replace cement in concrete manufacturing partially has the potential to be widely used in building and construction.

However, current studies still have limitations that prevent the concrete containing CWP from being widely used. For instance, the changes in two physical properties are unclear: strength development during curing and thermal insulation at elevated temperatures. Generally, faster strength development in concrete can reduce construction time and cost [11], and improved thermal insulation at elevated temperatures is essential for concrete to be used in high-temperature environments such as kilns, steam pipe construction, nuclear power plants, and metalworking facilities. Some conflicting findings are reported in the literature regarding the strength development of concrete. For example, Raval, Patel and Pitroda [8] indicated that partially replacing cement with CWP did not affect the strength development of concrete, with compressive strength at 7 days remaining around 78 % of that at 28 days with and without CWP. Taher, Abed and Hashim [12] reported that replacing cement with CWP prevented the development of concrete strength after 7 days of curing. Chen, Zhang, Cheng, Xu, Zhao, Wang, Wu and Bai [13], however, reported a contradictory finding. These inconsistent results warrant more studies in the subject area of strength development of modified concrete formulations. Also, to our knowledge, no studies have quantified changes in the thermal insulation of concrete at elevated temperatures when CWP partially replaces cement.

As mentioned earlier, contradictory results have been reported regarding the development of early-stage concrete strength and the changes in 28-day strength when CWP replaced cement. This is because there is a lack of basic understanding of the effect of CWP on the concrete mixture at the microstructural level. Microstructural features of concrete, including the porosity, degree of cement hydration, and the level of pozzolanic and alkali-silica reactions (ASR), affect the concrete strength development and thermal insulation behaviour. However, the effect of CWP on these features has not been well-studied. Some studies quantified the effect of CWP on concrete porosity by estimating the pore volumes in concrete using indirect methods such as Mercury Intrusion Porosimetry (MIP), as reported by El-Dieb, Taha and Abu-Eishah [14] and Awoyera, Akinmusuru, Dawson, Ndambuki and Thom [15]. However, MIP can only measure concrete porosity based on open pores and cannot focus on the interfacial transition zone (ITZ), where defects and cracks are likely to occur [16]. Therefore, porosity measurement at ITZ can only be achieved by more direct methods (e.g., as back-scattered-electron (BSE) image analysis), and these direct methods are not reported in the case of concrete containing CWP.

Additionally, Thermogravimetric analysis (TGA), X-ray diffraction (XRD) and Energy-dispersive X-ray spectroscopy (EDS) are useful techniques for estimating the degree of hydration and the level of pozzolanic and alkali-silica reaction (ASR). However, these techniques are rarely used for concrete containing CWP. TGA and XRD analyses were performed by Kannan, Aboubakr, El-Dieb and Taha [7] for concrete containing CWP. However, these lacked quantitative estimates of hydration products and comparisons of peak positions for different phases (such as C-S-H, Portlandite, Ettringite and Calcite) in TGA and XRD analyses. These studies primarily focused on estimating the pozzolanic and ASR reactions' level. Li, Liu, You, Chen and Zeng [17] and Mohit, Haftbaradaran and Riahi [18] performed the TGA and XRD analysis on mortars containing CWP, and found that adding CWP can contribute to pozzolanic reaction. However, the level of pozzolanic reaction in concrete can differ from that in mortar, as Tan and Tang [19] indicated that coarse aggregate in concrete can also affect chemical reactions, especially cement hydration in concrete.

Another knowledge gap in the current study is that the changes in concrete properties when CWP partially replaced cement against other SCMs, such as silica fume (SF), fly ash (FA), and slag, are not compared at both macro- and micro-scales. CWP has a similar grain size and contains a higher level of silica oxide than FA (both class C and F) and slag [3,20,21]. Therefore, it is expected that adding CWP in concrete can enhance the pozzolanic reaction, leading to lower concrete porosity, faster concrete strength development and better thermal insulation properties than FA and slag in concrete. However, there is insufficient evidence to demonstrate such enhancements, as comparisons between the macro- and micro-properties of CWP concrete and concrete containing other SCMs are lacking. This can prevent CWP concrete form from being widely used.

Therefore, this paper was intended to address the above-mentioned gaps and follow the changes in concrete properties, both at the macro- and micro-scales, when cement was partially replaced with CWP. Here, the focus was to measure the properties of concrete at the macro-scale —such as strength development and thermal insulation at room and elevated temperatures —and at the micro-scale, to gauge porosity, cement hydration degree, and levels of pozzolanic and alkali-silica reactions. The collated properties of CWP-concrete mixes were then compared with those of concrete using SF, FA, and slag as cement replacements, as reported in other studies. The main outcome of the present work is expected to inform, guide and promote sustainable concrete design by using CWP as a suitable replacement material for concrete manufacturing and the construction industries.

2. Experiment methods

Experiments were designed to measure the properties of concrete test specimens at the macro- and micro-levels. At the macro-level, the strength development and the thermal insulation attributes were determined by measuring the strength of CWP concrete samples

at different curing ages, and the thermal conductivity when exposed to different temperatures. At the micro-level, a scanning electron microscope (SEM with a Backscatter Electron Detector: BSE and provision for Energy Dispersive Spectroscopy: EDS), XRD and TGA were employed. The porosity, degree of hydration, and extents of pozzolanic and ASR reactions were assessed through these SEM, XRD and TGA analysis. Grade M40 concrete, a grade commonly used for slabs, beams, columns, and footings, was selected for the experiment, and CWP was used to replace 0, 10 %, and 20 % of the cement. The test design is shown in Fig. 1.

2.1. Materials

The CWP was obtained from the final cutting and polishing process of ceramic products from a local ceramic tile manufacturing, and the details of concrete manufacturing can be found in Li, Joseph, Zhang and Zhang [3]. Specifically, the concrete's water-cement ratio was kept at 0.40, and CWP was used as the cement replacement with replacements (by wt.) of 0, 10 %, and 20 % of Portland cement, respectively. The chemical composition of CWP and cement has been are shown in Table 1, based on the Li, Joseph, Zhang and Zhang [3], Alabadan, Njoku and Yusuf [22] and Cherop, Kiambi and Kosgey [23].

The maximum replacement ratio of 20 % was determined based on a preliminary study by Li, Joseph, Zhang and Zhang [3], which found that concrete strength begins to decrease at 20 % due to the excessive amount of CWP's degradation effect on the bonding strength between cement and aggregate. Nonetheless, future studies will examine the effect of CWP on concrete performance when the replacement ratio exceeds 20 %.

Natural crushed stone and sand were used as the coarse and fine aggregates, respectively, and the preparation for concrete followed AS1012.2 [24]. All concrete specimens were manufactured in cylinders 100 mm in diameter and 200 mm in height, and they were further cut to appropriate sizes for thermal conductivity analysis, and relatively smaller/powdered samples were employed for SEM image analysis, TGA and XRD tests.

2.2. Concrete compression test and strength development analysis

The compression tests followed AS1012.9 [25]. The specimens were conditioned at a fixed temperature (ca. 23 ± 2°C), in lime-saturated water, until 7, 14 and 28 days of curing. The curing set-up of concrete specimens is given in Fig. 2. After each curing period, three specimens were collected for compression tests, where the strength development during different curing periods at each CWP replacement level was monitored. Compressive strength for each mixture was quoted as an average value over three measurements on the cylindrical specimens, with the test plan summarized in Table 2. The load was performed continuously at a rate of 14 N/mm^2 per minute through a Universal Testing Machine (UTM) until failure, and the maximum load carried by the specimen were recorded.

2.3. Thermal conductivity test

A Transient Plane Source (TPS) method was used to investigate the thermal conductivity and thermal diffusivity of concrete containing different levels of CWP. The test followed ISO standards [26] through a hot disk thermal constant analyzer (Fig. 3). The test

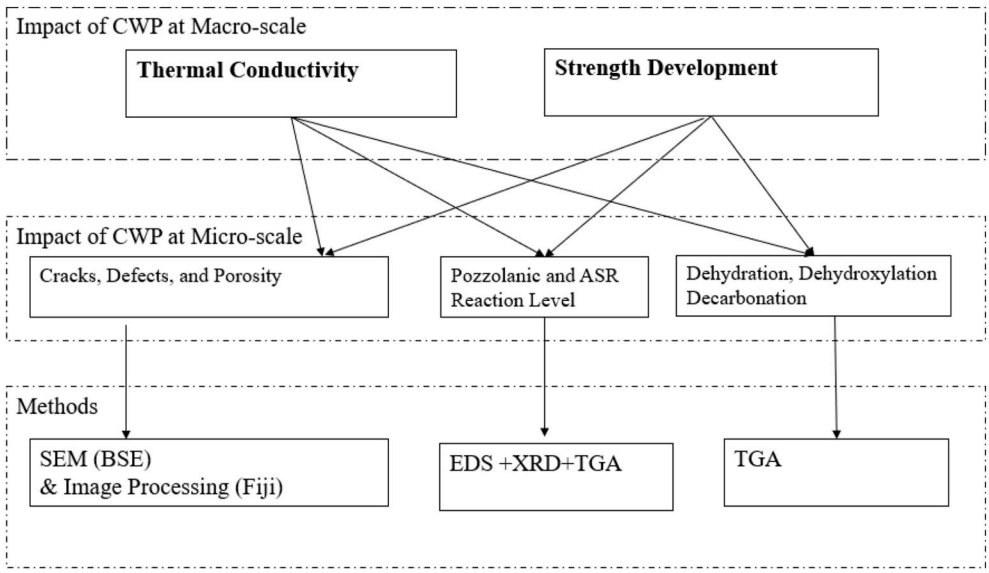

Fig. 1. A schematic representation of the experimental techniques used in this study for investigating the macro- and micro-structural properties of concrete with WPC.

Table 1
Chemical/Mineral composition of CWP and cement.

CWP		
Chemical name	Chemical formula	Weight Percentage (%)
Silicon dioxide	SiO_2	70.00
Aluminium oxide	Al_2O_3	18.30
Potassium oxide	K_2O	3.950
Sodium oxide	Na_2O	2.760
Ferric oxide	Fe_2O_3	1.400
Magnesium oxide	MgO	0.690
Titanium oxide	TiO_2	0.660
Calcium oxide	CaO	0.580
Cement		
Chemical name	Chemical formula	Weight Percentage (%)
Alite	$3CaO{\cdot}SiO_2$	54.65
Belite	$2CaO{\cdot}SiO_2$	25.60
Tricalciumaluminate	$3CaO{\cdot}Al_2O_3$	11.56
Tetracalcium Aluminoferrite	$4CaO\ Al_2O_3{\cdot}Fe_2O_3$	0.700

Fig. 2. Setup and curing of concrete samples.

Table 2
CWP concrete test plan.

Concrete	Replacement (%)	Curing time	Compressive strength test	Thermal conductivity test	Microstructural analysis (SEM, EDS, XRD, TGA)
Control	0	7	3	–	–
		14	3	–	–
		28	3	3	3[a]
	10	7	3	–	–
		14	3	–	–
		28	3	3	3[a]
	20	7	3	–	–
		14	3	–	–
		28	3	3	3[a]
Total specimen		45			

[a] Note: the three samples at each CWP replacement level are further cut nine samples for SEM and EDS analysis and grinded into powders for XRD and TGA analysis.

setup can be found in Li, Joseph, Zhang and Zhang [3] and shown in Fig. 3. Three concrete specimens were used for the tests at each CWP replacement level (Table 2), and results are quoted by taking the average of the three measurements. The changes in thermal conductivity and thermal diffusivity against temperature were also determined at different CWP replacement levels.

Each specimen was cut into two samples of 10 mm thickness and dried in an oven set at 105 ± 5°C for 24 h. The hot disk sensor was then sandwiched between two samples to act as a heat source and a temperature probe, and the samples were heated at 25°C, 75°C, 12°C and 175°C to measure the thermal conductivities and thermal diffusivities. Notably, heating the samples to 175°C can simulate the concrete exposed to high-temperature environments such as furnace linings, kilns, or steam pipe construction [27].

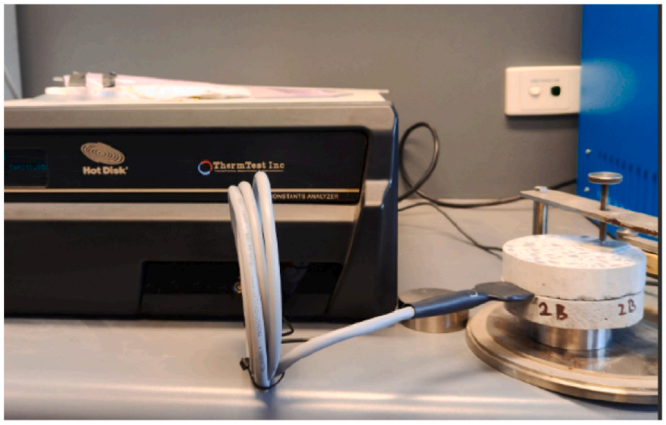

Fig. 3. Thermal conductivity tests on the samples.

2.4. SEM and image analysis

Concrete samples were cut from the cylinder specimens (Table 2) into a shape of 40 × 20 × 10 mm. The samples were collected approximately mid-distance from the centre to the edge, and nine samples were collected from each one, including the CWP- replaced versions.

The cut samples were freeze-dried and cleaned according to ASTMC1723-16 [28]. They were then cold-mounted with epoxy resins (Fig. 4) and polished using Silicon Carbide grinding papers (180, 400, 600, and 1200 grits) and 3 μm diamond paste, with a 7 N force applied to each specimen. Samples were then cleaned ultrasonically in acetone and coated with a carbon layer using an evaporative coater before SEM analysis.

The SEM analysis was carried out using the FlexSEM 1000 equipped with a Backscatter Electron Detector (BSE) at the University of Melbourne. A working distance of 10 mm and an accelerating voltage of 10 kV were used to operate the microscope. Sixty images were taken across the nine samples at each CWP replacement level, and the magnification was set at × 50. Initially, a quick SEM scanning was performed, and most of the pores and defects can be found in the concrete's interfacial transition zone (ITZ). Subsequently, sixty SEM images were taken at the ITZ to yield a conservative estimation of the concrete porosity. Here, areas near the sample edge were not imaged to avoid the defects that were caused by the saw during the sample-cutting procedure.

The BSE-SEM image analysis was performed using the software ImageJ/FIJI to determine the concrete porosity, following Edwin, Mushthofa, Gruyaert and De Belie [29] and Song, Dai, Zhou, Bian, Zhao and Song [30]. The scale of SEM images was adjusted based on the scale bar, and the maximal overlapped area was cropped for image analysis. Afterwards, a background filter, FFT filter and "Median 3D″ filter were applied to the images to remove the shadow effect, water curtain effect and "salt and pepper" noises, respectively [31]. Fig. 5 shows the image processing steps for the SEM image captured for concrete with 20 % cement replaced by CWP. It is worth noting that circular cracks have been found in the concrete cement in Fig. 5. This crack is likely to form due to ASR, which is caused by the presence of silica and sodium in concrete. The reaction can exert pressure on voids and defects within concrete, leading to tensile stress and internal cracking.

Afterwards, the SEM images were segmented using the Otsu algorithm considering their stable segmentation effect. Zheng, Gao, Zhang, Lei and Zhang [32] indicated that the Otsu algorithm may perform poorly in case of heavy noise and small object size. Thus, all the segmentation images generated by the Otsu algorithm were inspected and edited manually.

After pore segmentation, the volume, perimeter and the number of pores (including voids, cracks, and defects) can be measured by the ImageJ/FIJI software, and the porosity (ϕ_p), average pore size $\overline{A}$, and circularity C of concrete for each SEM image can be determined as follows [33,34]

$$\phi_p = \frac{\sum A}{\sum A_P} \tag{1}$$

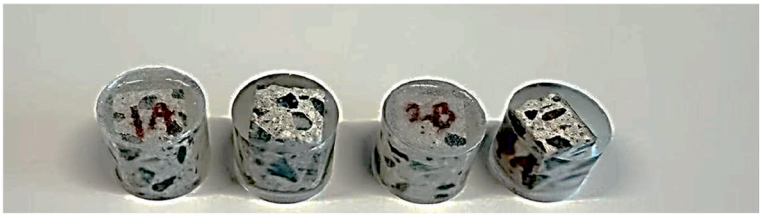

Fig. 4. SEM and image analysis of samples.

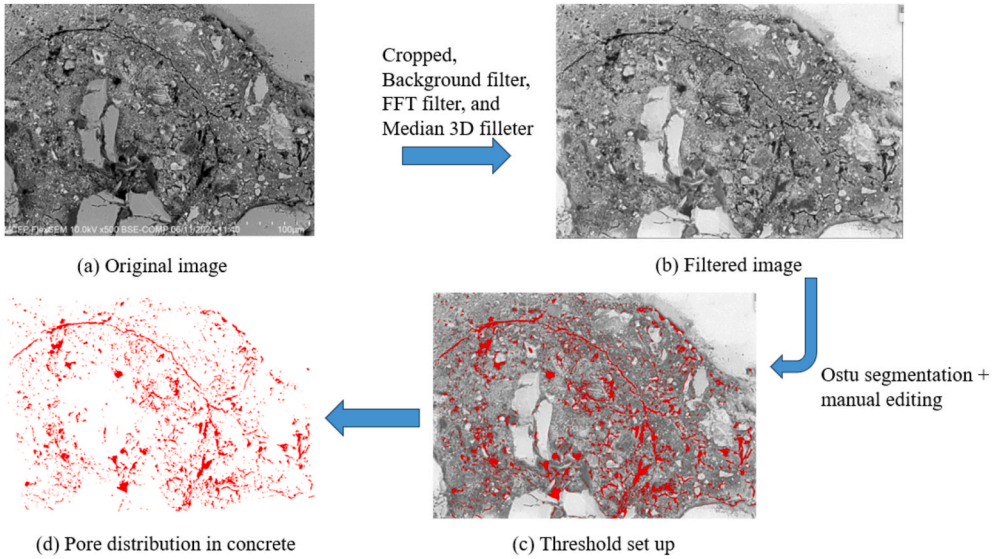

Fig. 5. BSE-SEM image processing and thresholding technique used for segmentation and quantitative porosity analysis.

$$\overline{A} = \frac{\sum A}{num} \tag{2}$$

$$C = 4\pi \frac{\sum A}{(Perimeter)^2} \tag{3}$$

where A and A_P are measured areas of the pores and concrete. Here, *num* is the total number of pores and *Perimeter* is the total perimeter of pores on each SEM image.

2.5. Energy dispersive spectroscopic (EDS) analysis

After BSE-SEM image capturing and analysis, as given in Section 2.4, the accelerating voltage of FlexSEM was changed to 15 kV and the magnification was increased to 1000× to find the possible pozzolanic and ASR reactions' products. The EDS map (over SEM captured images) and point analyses (over possible products) were then carried out to check the existence of pozzolanic and ASR reactions for concrete specimens with and without CWP.

2.6. XRD and TGA

XRD and TGA analyses were carried out on concrete specimens, at each CWP replacement level, after 28 days of curing and compression tests (in Section 2.1). The middle fragments from the core of the specimen, excluding coarse aggregates, were collected. These fragments were finely ground, sieved through a 90 μm sieve to produce a fine powder, and dried in the oven at 40–45°C. X-ray diffraction (XRD) analyses were carried out on these fine powders at the University of Melbourne to assess the chemical and phase composition of concrete at different CWP replacement levels.

TGA runs were also performed on these fine powders under an atmosphere of nitrogen using the Thermogravimetric Analyzer at Victoria University (Mettler-Toledo TGA/DSC1Star), in which the powders were heated up through the following steps [35].

- 30°C–45°C at 10°C per minute
- Hold temperature at 45°C for 15 min to expel any moisture
- Heat from 45°C to 850°C at 10°C per minute

The mass loss of concrete powder through the various temperature ranges was recorded throughout the analysis to assess the degree of pozzolanic reactions and cement hydration.

3. Results and discussion

3.1. Strength development

The compression test results for each concrete with CWP replacing 0, 10 % and 20 % cement are shown in Fig. 6. It can be seen from Fig. 6a that the compressive strength of concrete when CWP replaces 10 % and 20 % of cement at 7 and 14 days of curing time is higher than the strength of concrete without CWP. Fig. 6b shows that the compressive strength at 7 and 14 days reaches 89.5 % and 92.3 % of the strength at 28 days for concrete when CWP replaces 10 % of cement. These two percentages increase slightly to 90.7 % and 97.9 % when CWP replaces 20 % cement. However, when no CWP replaces cement, concrete's compressive strength at 7 and 14 days only reaches 69.9 % and 82.0 % of the strength at 28 days. Thus, adding CWP to concrete can accelerate the strength development rate, thereby decreasing the construction time used in practice.

The ultrafine particle size of CWP can possibly fill the voids and densify the concrete microstructures, thereby contributing to the strength development. CWP also contains a high level of silicon dioxide (SiO_2), which can also lead to rapid pozzolanic reaction and improvement in the strength development rate by forming C-S-H and C-A-H gels [36], with reaction details as shown below:

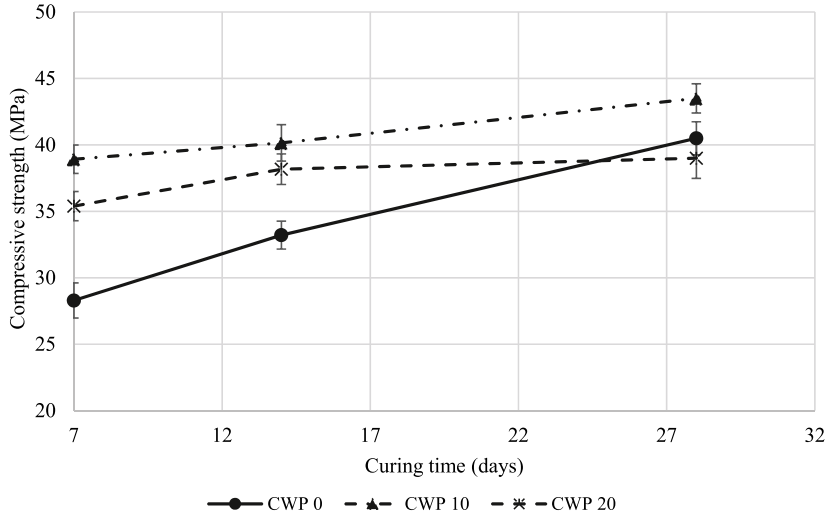

(a) Compressive strength of samples over curing time

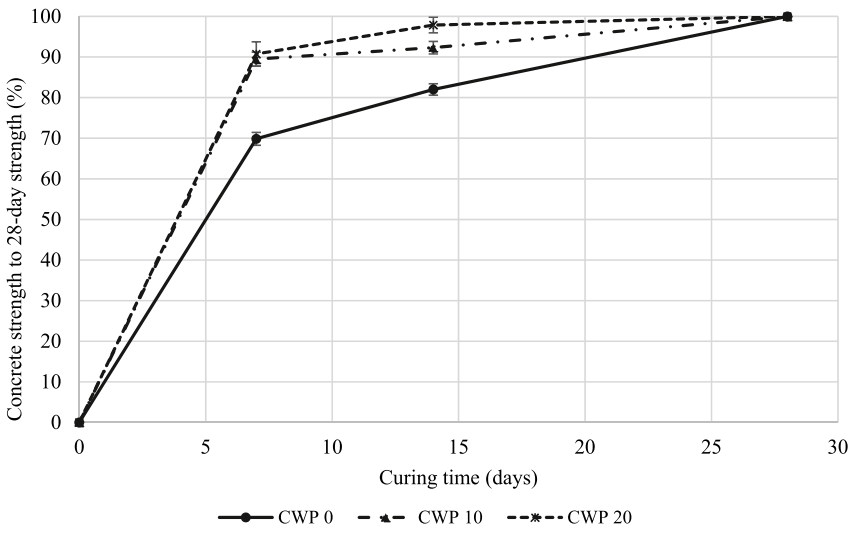

(b) Percentage of concrete strength gained relative to its 28-day strength during curing

Fig. 6. Strength development of concrete with CWP replacing different levels of cement.

$$3Ca(OH)_2 + 2SiO_2 \rightarrow 3CaO \cdot 2SiO_2 \cdot H_2O \quad (C-S-H)$$

$$3Ca(OH)_2 + Al_2O_3 + 3H_2O \rightarrow 3CaO \cdot Al_2O_3 \cdot 6H_2O \quad (C-A-H)$$

The evidence of void-filling effect and rapid pozzolanic reaction is revealed later in the microstructural analysis. Additionally, CWP, like other SCMs, can reduce the ASR reaction by binding alkalis and reducing alkali concentration in concrete pores [37], which can also lead to faster strength development.

Fig. 6a also shows that at each curing time, the compressive strength increases with increasing CWP content to a peak level when CWP replaces 10 % of cement and then decreases with further additions. The finding indicates that although adding CWP can promote the pozzolanic reaction, excessive CWP would still reduce the compressive strength. This may be because excessive CWP particles can affect the bonding between concrete cement and aggregate, thus making the concrete vulnerable to cracking under compression. From the compressive strength and strength development perspectives, replacing 10 % of cement with CWP can achieve the highest strength at each curing time and a relatively faster strength growth rate. The changes in 28-day compressive strength for concrete are within the acceptance tolerance (±15 %) when CWP replaces 20 % cement. As specified in ACI 318–19 [38], the ±15 % tolerance requires that no individual compressive strength fall below $f'_c - 0.15f'_c$. For the control concrete (40.5 MPa), this corresponds to 34.4 MPa ($40.5 - 0.15 \times 40.5 = 34.4\,MPa$). The mix with 20 % CWP achieved 39 MPa (minimum 37 MPa), exceeding this limit and indicating no significant strength reduction. The concrete with 20 % CWP, which replaces cement, can still be treated as M40 grade concrete for practical use [10].

As mentioned in the introduction, SF, FA and slag (such as Ground Granulated Blast-Furnace Slag-GGBS and Blast Furnace Slag-BFS) are other common SCMs used to replace cement in concrete manufacturing. Popovics and Ujhelyi [39] and Knight, Cunningham and Miller [40] highlighted three significant factors affecting concrete strength development: the replacement level of SCMs, the elemental composition of SCMs and the water-cement ratio (w/c). Table 3 compares the strength development for concrete containing CWP and other SCMs with the information on three influence factors summarized. In particular, the elemental composition focused on SiO_2, Al_2O_3 and CaO contents, which are critical for the pozzolanic reaction.

Table 3 shows that the strength development of CWP concrete can be similar to that of SF concrete at the same cement replacement level. For example, the strength of CWP concrete at 7 days can reach 89.5 % of that at 28 days at a cement replacement level of 10 %, and the corresponding value is 77.0–88.0 % for SF concrete. This is likely because both CWP and SF contain a higher level of SiO_2 that can contribute to a rapid pozzolanic reaction. Table 3 also shows that the strength development for CWP concrete is faster than FA and slag concrete at the same cement replacement. The strength of FA (including both Class C and F) concrete at 7 days is only 76.0 % of that at 28 days with 10 % cement replacement. For slag concrete, the strength at 7 days to that of 28 days ranges from 68.9 to 71.7 % when slag replaces 15–30 % cement, and this percentage is 90.7 % for CWP concrete at a cement replacement ratio of 20 %. This is because FA and slag have a lower level of SiO_2 than CWP.

The influence of cement replacement level, SiO_2, Al_2O_3, CaO contents of SCMs, and the water–cement ratio on the 28-day strength

Table 3
Comparison of strength development of concrete containing different SCMs.

	Replacement	Cement Replacement level (%)	SiO_2 (%)	Al_2O_3 (%)	CaO (%)	w/c	Strength at 7 days (% to 28 days)	Strength at 14 days (% to 28 days)
This study	CWP	10	70.00	18.30	1.40	0.45	89.5	92.3
	CWP	20	70.00	18.30	1.40	0.45	90.7	97.9
Mazloom,	SF	6	90.71	1.000	1.68	0.35	77.7	89.2
Ramezanianpour and	SF	10	90.71	1.000	1.68	0.35	77.0	90.3
Brooks [41]	SF	15	90.71	1.000	1.68	0.35	75.7	90.0
Wong and Razak [42]	SF	5.0	92.06	0.480	0.40	0.27	85.3	–
	SF	10	92.06	0.480	0.40	0.27	82.7	–
	SF	15	92.06	0.480	0.40	0.27	75.7	–
	SF	5.0	92.06	0.480	0.40	0.30	89.0	–
	SF	10	92.06	0.480	0.40	0.30	82.6	–
	SF	15	92.06	0.480	0.40	0.30	75.6	–
	SF	5.0	92.06	0.480	0.40	0.33	83.7	–
	SF	10	92.06	0.480	0.40	0.33	78.8	–
	SF	15	92.06	0.480	0.40	0.33	80.0	–
Behnood and Ziari [43]	SF	6.0	91.70	1.680	1.00	0.35	83.2	–
	SF	6.0	91.70	1.680	1.00	0.30	86.1	–
	SF	10	91.70	1.680	1.00	0.30	88.0	–
Saha, Pan and Pan [44]	FA (Class F)	20	58.15	22.67	1.23	0.38	75.0	–
	FA (Class F)	20	58.15	22.67	1.23	0.27	54.7	–
	FA (Class F)	30	58.15	22.67	1.23	0.27	62.5	–
	FA (Class F)	40	58.15	22.67	1.23	0.27	57.1	–
Chindaprasirt and Rukzon	FA (Class C)	10	41.10	21.60	14.40	0.50	76.0	–
[45]	FA (Class C)	20	41.10	21.60	14.4	0.50	74.8	–
	FA (Class C)	40	41.10	21.60	14.4	0.50	58.4	–
Oner and Akyuz [46]	Slag (GGBS)	15	39.20	10.20	32.8	0.10–0.20	70.2–71.7	74.0–79.2
	Slag (GGBS)	30	35.00	16.00	40.0	0.10–0.20	68.9–71.5	74.0–79.0

variation was examined. Correlation coefficients (r) were determined between each factor and the 28-day strength change, defined as the percentage difference between SCM and control concretes in Table 3. The equation to determine the correlation coefficient (r) is shown below [47]:

$$r = \frac{Cov(x,y)}{\sigma_x \sigma_y} \tag{4}$$

where $Cov(x,y)$ is the covariance of x and y, x represents the cement replacement levels, SiO_2, Al_2O_3 and CaO contents of SCMs, and the water-cement ratio, and y represents the strength development at 7 days. Here, σ_x and σ_y are the standard deviations of x and y.

Cement replacement levels and SiO_2 and Al_2O_3 contents in SCMs have a higher correlation strength than other factors. A negative correlation has been found between cement replacement levels and 28-day strength changes. Adding too much SCM can affect the bonding between concrete cement and aggregate. Also, a negative correlation has been found between Al_2O_3 content of SCMs and 28-day strength changes. Although Al_2O_3 can contribute to pozzolanic reaction, an extra high amount of Al_2O_3 content can affect the stiffening of cement paste [48]. Table 4 confirms a strong and positive correlation between SiO_2 and 28-day strength changes, as SiO_2 can contribute to the pozzolanic reaction.

3.2. Thermal conductivity

Fig. 7 shows the thermal performance of concrete with and without CWP. Replacing cement with CWP can improve the thermal performance of concrete, both at room and elevated temperatures. There is an 11.2 % and 13.6 % reduction in thermal conductivity and thermal diffusivity when CWP replaces 20 % cement at room temperature. As Li, Joseph, Zhang and Zhang [3] have demonstrated, the void-filling impact of CWP can convert big voids/defects in concrete into a few smaller ones (evidence shown later in the SEM analysis). Shells of protected cement paste surround these voids, and an increasing number of small air voids can increase the shells' thickness and the thermal insulation of concrete. The formation of C-S-H gels due to pozzolanic reaction also has a lower thermal conductivity than cement and aggregates [49]. Thus, their existence can reduce the thermal conductivity of concrete.

Fig. 7 also shows that the thermal conductivity of concrete with and without CWP reduces with temperature increase. An increasing temperature can lead to concrete spalling, defect formation, and crack growth and propagation. It can also be seen from Fig. 7 that when temperature increases from 25 °C to 175 °C, the thermal conductivity of concrete reduces by 50.2 %, 45.6 %, and 46.8 % when CWP replaces 0, 10 % and 20 % cement. The corresponding percentages are 82.2 %, 79.1 % and 79.7 %, respectively, for thermal diffusivity. There is less reduction in thermal conductivity and diffusivity when temperature increases for the concrete containing CWP. Presumably, an increased number of C-S-H gels can prevent the defect formation of concrete and lead to a more stable thermal performance than concrete without CWP. Here again, these reductions for concrete containing 10 % CWP are smaller than those for concrete containing 20 % CWP, indicating that excessive CWP particles can affect the bonding between concrete, cement and aggregate.

Table 5 compares the strength development for concrete containing CWP and other SCMs at room temperature, and the tables show that adding various SCMs can reduce the values of thermal conductivity. The thermal conductivity reduction of CWP concrete at a replacement level of 10 % is 5.6 %. This value is 3.2–7.1 % for SF concrete, 10.9 % for FA-containing concrete and 3.8–11.1 % for slag-containing concrete at a replacement level of 10 %. The mechanisms of thermal conductivity reduction are similar across these SCMs (void-filling effect and pozzolanic reaction). To be specific, the void-filling effect can reduce pore size and water mobility, thereby increasing the stability of entrapped air in micro voids. The thermal resistance of concrete can thus be increased due to the low thermal conductivity of the entrapped air, as indicated by Shah, Yuan and Zuo [50], Lakhiar, Kong, Bai, Susilawati, Zahidi, Paul and Raghunandan [51], and Lallas, Gombeda and Mendonca [52]. The pozzolanic reaction can also reduce the pore size of the concrete and increase the stability of entrapped air [53]. Additionally, the pozzolanic reaction product (C-S-H gels) has lower thermal conductivity than cement, which can increase concrete's thermal resistance [54]. Although there can be a potential increase in concrete overall porosity for SF-, FA- and slag-containing concrete (evidence shown later in Table 7), the existence of SCM particles can still fill them and large pores/cracks into smaller ones, and thus increase the shell thickness that protects the cement paste and the stability of entrapped air.

Correlation coefficients (r) were calculated for different influencing factors against the thermal conductivity based on Equation (4), and are collected data in Table 5, with the corresponding results shown in Table 6. Table 6 also shows that thermal conductivity values correlate more strongly with CRL, SiO_2, and CaO contents than other factors. Increasing CRL can contribute to void-filling effect and the pozzolanic reaction. Also, most of the CRL summarized in Table 5 is less than 30 %, and thus the reduction in bonding between cement and aggregate due to the excessive amount of CRL is not obvious, leading to a negative correlation between CRL and thermal

Table 4
Correlation of different factors against the 28-day strength changes.

Correlation item		Correlation coefficient	Correlation strength	Correlation type
Cement Replacement Level (CRL, %)	28-day strength changes	−0.72	Strong	Negative
SiO_2 content (c_{sio_2}, %)		0.73	Strong	Positive
Al_2O_3 content ($c_{Al_2O_3}$, %)		−0.83	Very Strong	Negative
CaO content (c_{CaO}, %)		0.22	Weak	Positive
water cement ratio (w/c)		−0.12	Weak	Negative

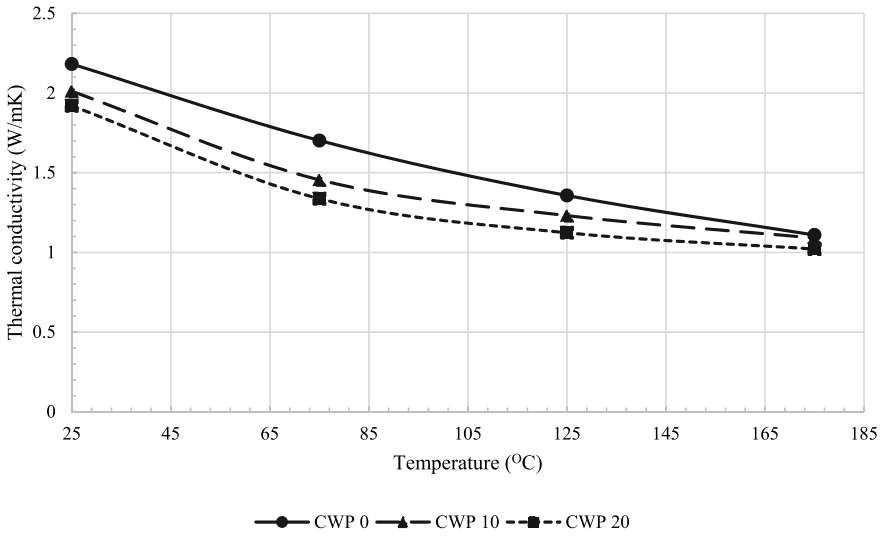

(a) Thermal conductivity

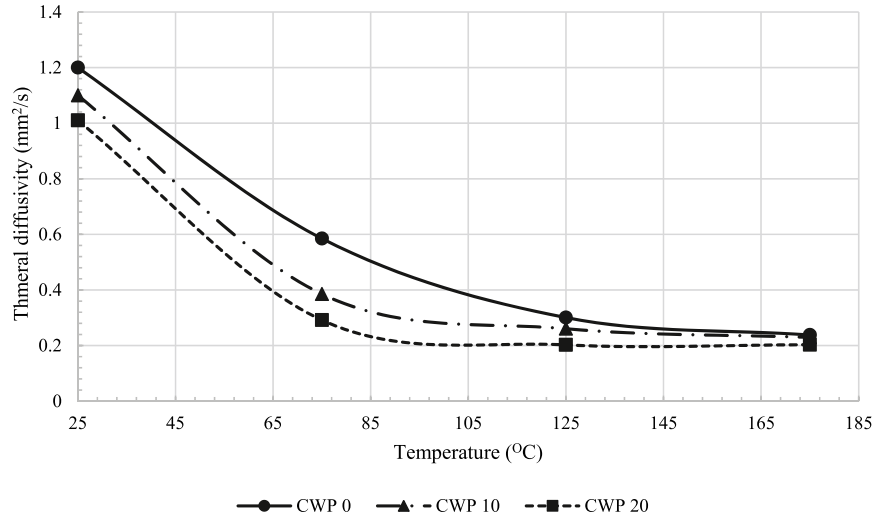

(b) Thermal diffusivity

Fig. 7. Thermal performance concrete with varying CWP contents at different temperatures.

conductivity. Furthermore, SiO_2 content increment can encourage the formation of C-S-H gels, and thus there is also a negative correlation between SiO_2 and thermal conductivity. On the contrary, an increasing CaO content in concrete can hinder the pozzolanic reaction. There is a also positive correlation between Cao content and thermal conductivity.

3.3. Porosity of concrete

Fig. 8 shows the BSE-SEM images of concrete containing different levels of CWPs. Adding CWP can reduce the concrete's porosity and densify its microstructure at the interfacial transition zone (ITZ). The CWP's void-filling effect and rapid pozzolanic reaction can also lead to this reduction in concrete porosity. Fig. 8 also indicates that adding CWP can reduce ASR reaction, as ASR can increase the number of pores and cracks in concrete by forming expansive gels.

Fig. 9 summarizes the average porosity, pore size, and circularity with the sixty frames (i.e., the sixty images were taken across the nine samples) at each CWP replacement level, and results further confirm that there is a reduction in porosity and pore (including defect, cracks, and void) sizes at ITZ. The average porosity across the sixty frames is 22.7 %, 11.5 % and 8.9 % when CWP replaces 0, 10 % and 20 % cement, respectively, indicating a 60.8 % reduction in porosity when CWP replaces 20 % cement. Similarly, there can be an 86.3 % reduction in the pore sizes. The standard deviation in concrete porosity and pore size are 4.20 and 95.5, 1.60 and 10.3,

Table 5
Comparison of thermal conductivity of concrete containing different SCMs.

	Replacement	Replacement level (%)	SiO_2 (%)	Al_2O_3 (%)	CaO (%)	w/c	Thermal conductivity reduction (%)
This study	CWP	10	70.00	18.30	1.40	0.45	5.60
	CWP	20	70.00	18.30	1.40	0.45	11.2
Mostofinejad, Aghamohammadi, Bahmani and Ebrahimi [55]	SF	10	90.00–95.00	0.600–1.200	0.50–1.50	0.56	7.10
	SF	15	90.00–95.00	0.600–1.200	0.50–1.50		9.60
Narattha, Thongsanitgarn and Chaipanich [56]	FA (Class F)	30	45. 40	20.60	12.30	0.48	6.70
Zhao, Qu, Li and Wei [57]	Slag (BFS)	10	13.46	3.560	45.16	–	3.80–11.10
	Slag (BFS)	20	13.46	3.56	45.16	–	7.7–22.2
Demirboğa [20]	SF	7.5	93.70	0.30	0.35	0.35	5.3
	SF	15	93.70	0.30	0.35	0.35	13.8
	FA (Class C)	15	30.60	13.80	5.50	0.35	6.5
	FA (Class C)	30	30.60	13.80	5.50	0.35	19.7
	Slag (BFS)	15	30.56	10.82	0.33	0.35	10.6
	Slag (BFS)	30	30.56	10.82	0.33	0.35	15.4
Kim, Jeon, Kim and Yang [58]	FA (Class not specified)	50	–	–	–	0.47	6.0
	Slag (BFS)	50	30.56	10.82	0.33	0.42	10.0
Demirboğa and Gül [59]	SF	10	93.70	0.30	0.35	–	3.2
	SF	20	93.70	0.30	0.35	–	6.3
	SF	30	93.70	0.30	0.35	–	9.4
	FA (Class C)	10	30.60	13.80	5.50	–	10.9
	FA (Class C)	20	30.60	13.80	5.50	–	11.1
	FA (Class C)	30	30.60	13.80	5.50	–	12.5

Table 6
Correlation of different factors against the thermal conductivity.

Correlation item		Correlation coefficient	Correlation strength	Correlation Type
Cement Replacement Level (CRL, %))	Thermal conductivity	−0.55	Moderate	Negative
SiO_2 content (c_{sio_2}, %)		−0.55	Moderate	Negative
Al_2O_3 content ($c_{Al_2O_3}$, %)		0.15	Weak	Positive
CaO content (c_{CaO}, %)		0.61	Moderate	Positive
water cement ratio (w/c)		−0.05	Weak	Negative

Table 7
Comparison of porosity changes of concrete containing different SCMs.

	W/C	Replacement material	Replacement level (%)	Reduction in porosity (%)	Measurement
This study	0.45	CWP	10	3.9–75.0*[1]	SEM segmentation
			20	12.1–75.1*[1]	
Chinchillas-Chinchillas, Rosas-Casarez, Arredondo-Rea, Gómez-Soberón and Corral-Higuera [60]	0.35	SF	10	−50.0	
Poon, Kou and Lam [61]	0.30	SF	5.0	20.3	MIP
			10	28.5	
Luo, Hua, Liu, Sun, Yi and Pan [62]	0.48	SF	10	41.3	
Gonçalves Junior, Jussiani, Andrello, Vanderlei and Toralles [63]	0.54	Slag (BFS)	50	−17.0	
			75	−17.6	
			90	−30.7	
Attari, McNally and Richardson [64]	0.50–0.56	Slag (GGBS)	30	36.0	SEM segmentation
			50	12.9	
			70	−8.3	
Poon, Lam and Wong [65]	0.30	FA (Class F)*[2]	15	2.3	MIP
			25	15.3	
			45	−7.7	
			55	−23.1	
	0.50	FA (Class F)*[2]	15	2.8	
			25	−5.3	
			45	−10.5	
			55	−26.3	

*[1]The range is determined based on the lower and upper bounds of porosity reduction across the sixty frames, based on Fig. 9a.
*[2]Very limited studies are on Class C FA, and thus only Class F FA is summarized in table.

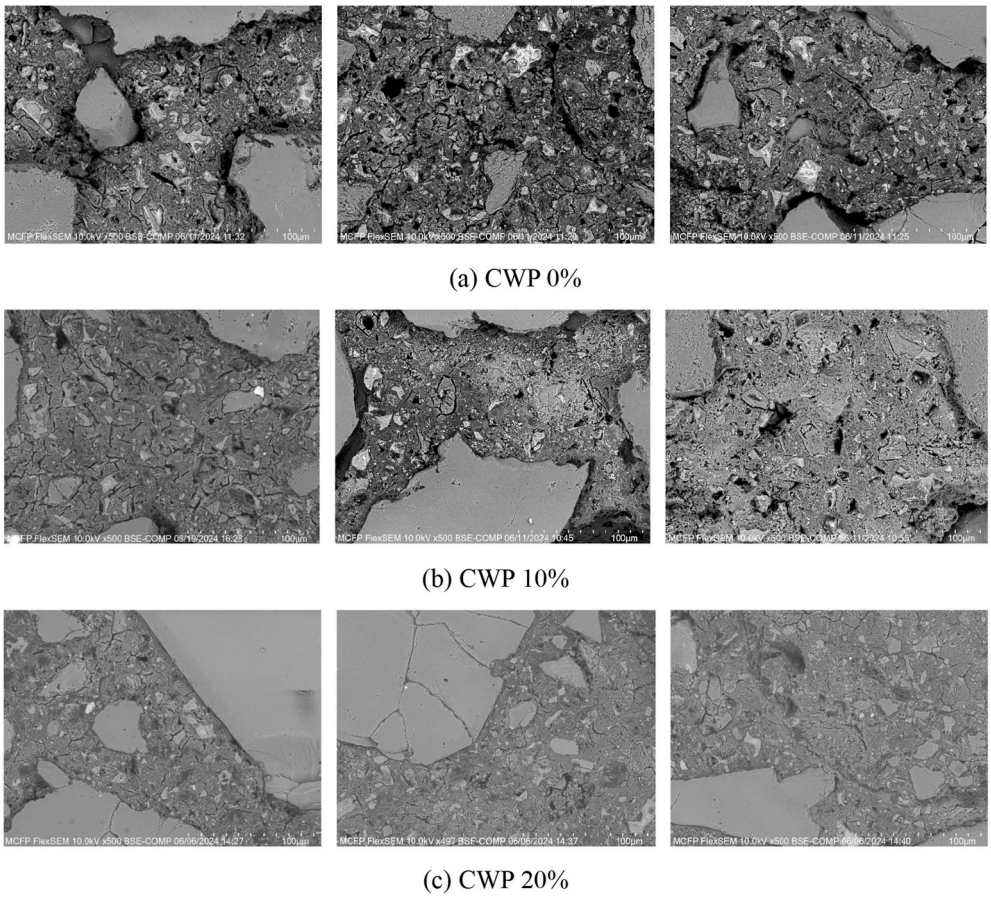

Fig. 8. Effect of CWP on microstructure of concrete (SEM analysis-porosity and cracks).

and 2.20 and 6.50 when CWP replaced cement 0, 10 % and 20 % cement, indicating that the pozzolanic reaction and void-filling effect caused by CWP leads to a stable pore size distribution and fewer defects and cracks across the concrete ITZ.

There is no noticeable difference in pore circularity, considering that the circularity can be very random within concrete, both with and without CWP.

Table 7 compares the porosity of concrete containing CWP and other SCMs. Unlike CWP concrete, there are contradictory findings on the effect of adding SF, FA, and slag on concrete's properties, indicating that the porosity changes can be susceptible to factors such as SCM types, cement and aggregate types, and water-cement ratio. More detailed investigations are needed to better quantify the influence(s) of these factors on concrete's porosity. Nevertheless, the comparison indicated that replacement cement using CWP can reduce the concrete porosity comparably to, or better than, other SCMs.

3.4. EDS analysis

In almost all SEM micrographs, Calcium Silicate Hydrate (C-S-H) gels usually show a lighter colour than surrounding pastes [66]. The C-S-H gels can be found and are highlighted in Fig. 10a–c and e for concrete with and without CWP. Point EDS was carried out at these highlighted locations, and results confirm the existence of C-S-H gels by finding a high percentage of silicon (Si) and calcium (Ca), as shown in Fig. 10b, d, and f (one among all highlighted locations was selected as a representative). The SEM-EDS analysis further confirms the occurrence of pozzolanic reactions in concrete with and without CWP. Also, a zoomed-in image of the C-S-H gels shows the existence of Portlandite [$Ca(OH)_2$] and Ettringite [$Ca_6Al_2(SO4)_3(OH)12{\cdot}26H_2O$] around the C-S-H gels due to cement hydration. The existence of Al_2O_3 in CWP can also lead to the formation of Ettringite. Vigil de la Villa Mencía, Frías, Ramírez, Carrasco and Giménez [67] have similar findings by investigating the products around C-S-H gels.

It is worth noting that SEM-EDS analysis only shows the occurrence of pozzolanic reactions and cannot quantify their level. The effect of CWP on the level of pozzolanic reactions can be quantified through TGA and XRD analysis, shown later in Sections 3.5 and 3.6.

Table 8 shows the EDS analysis of the entire SEM-scanned area of Fig. 10a–c, and e. It can be seen from Table 8 that there is a low percentage of sodium (Na) composition, and no potassium (K) was found through the EDS analysis. The existence of these two elements can be treated as evidence for ASR reactions [68]. Thus, the results show a low level of ASR reaction for concrete with and without CWP.

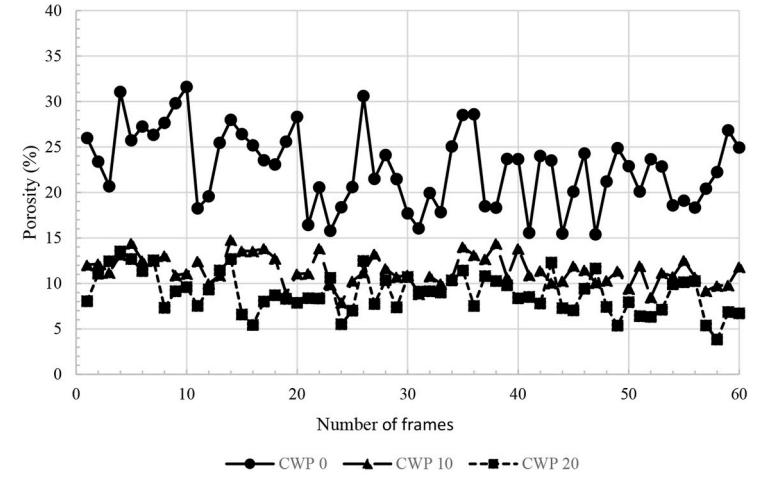

(a) Porosity

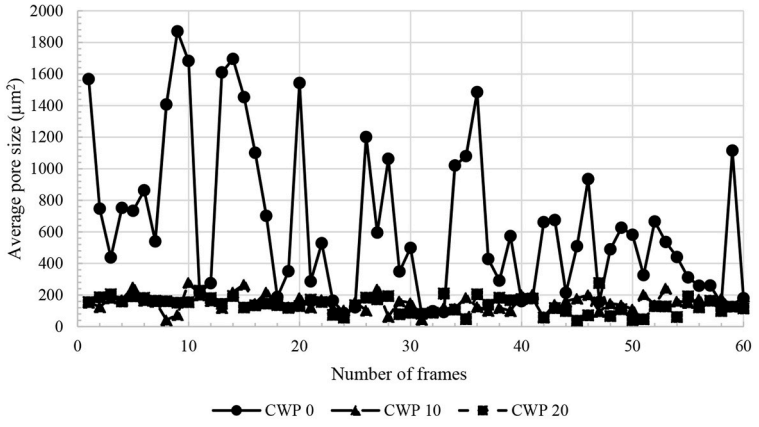

(b) Void size

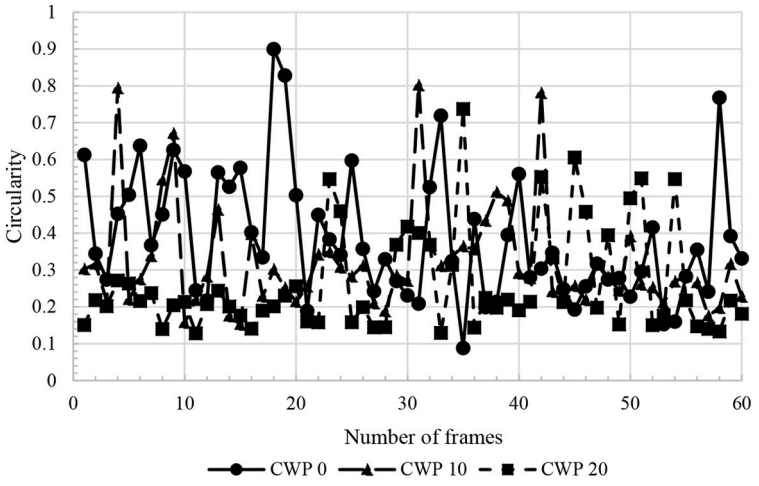

(c) Circularity

Fig. 9. Variation in porosity measurements with the number of analysed frames for concrete containing different CWP contents.

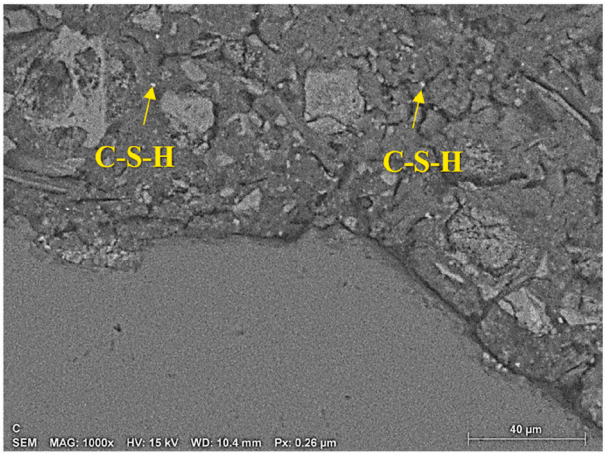

(a) CWP 0% (SEM analysis 1000 ×)

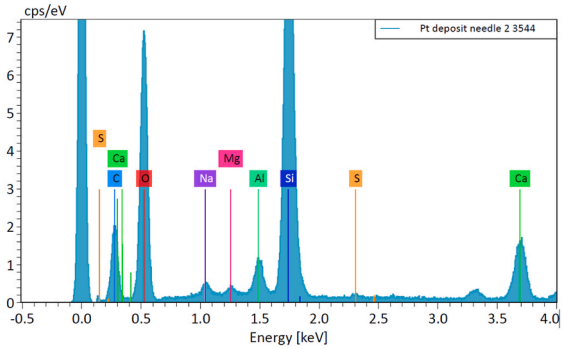

(b) CWP 0% (EDS analysis)

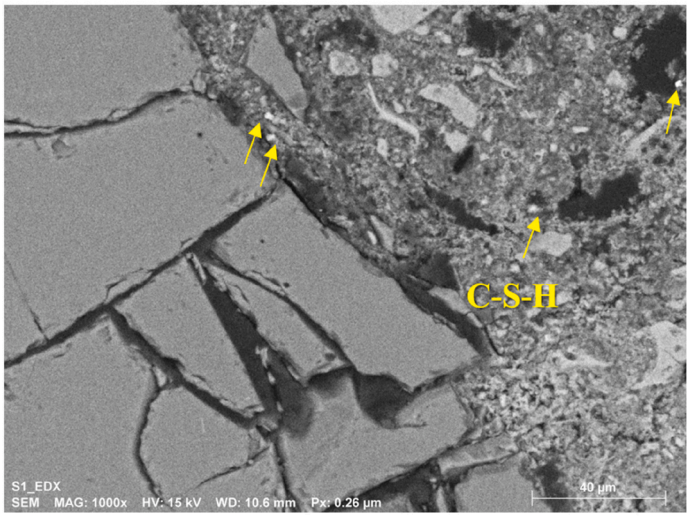

(c) CWP 10% (SEM analysis 1000 ×)

Fig. 10. SEM and EDS analysis of concrete samples containing different CWP contents

3.5. TGA results

Thermogravimetric analysis (TGA) results are shown in Fig. 11. All the samples that were tested had their thermal curves broken down into four steps: the first step is due to the loss of the water molecules; the second step is due to the decomposition of hydrates

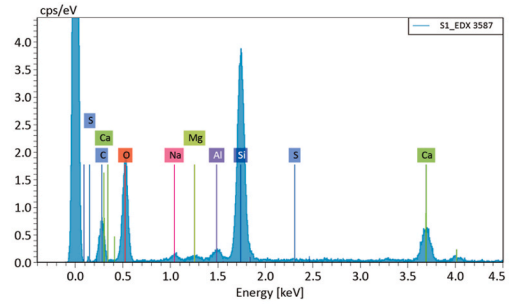

(d) CWP 10% (EDS analysis-point analysis)

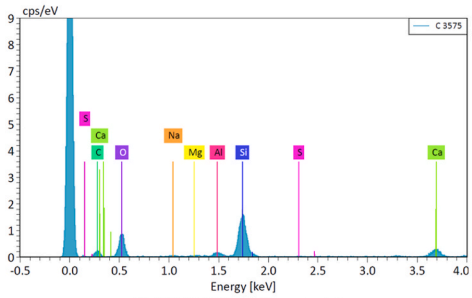

(f) CWP 20% (EDS analysis)

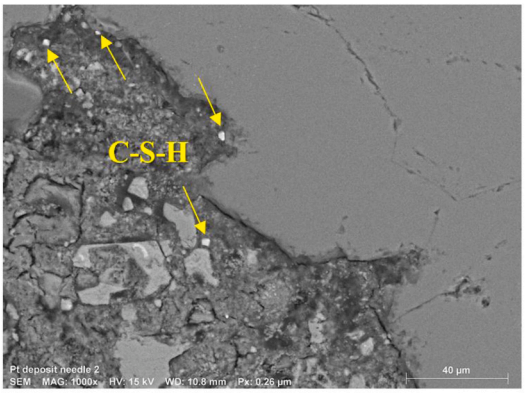

(e) CWP 20% (SEM analysis 1000 ×)

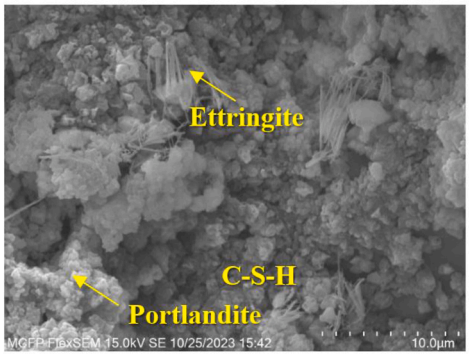

(g) Micrographs of C-S-H (SEM analysis 2000 ×, CWP 10% as a representative)

Fig. 10. (*continued*).

Table 8
Element composition captured through EDS mapping.

Element	Composition (%)		
	CWP 0	CWP 10	CPW 20
C[a]	27.24	26.64	27.20
O	42.28	42.24	42.72
Na	1.04	0.96	0.81
Mg	0.76	1.01	1.05
Al	1.73	1.75	3.05
Si	10.33	11.67	11.71
S	0.22	0.17	0.16
Ca	14.17	15.56	13.30

[a] It is only a rough estimation of the Carbon composition, considering that the Carbon spray was performed during the sample preparation.

(including the decomposition of C-S-H gels, Ettringite and other hydrate phases), namely dehydration (Ldh); the third step is due to the decomposition of Portlandite, namely dehydroxylation (Ldx); and the fourth step is the decarbonation (Ldc) of Calcite ($CaCO_3$) [56]. The temperature range for each step varies, and typical reported ranges can be found in Bhatty [69], Pane and Hansen [70] and Monteagudo, Moragues, Gálvez, Casati and Reyes [71], as shown in Table 9.

Fig. 11 also indicates that concrete with CWP decomposed to 73.4 % of its original mass at 850°C. Replacing cement with 10 % and 20 % CWP improves the decomposition to 77.9 % and 77.1 %. This increment is because adding CWP can result in a condensed cement matrix, leading to a better thermal stability. Also, the thermal stability is better for concrete containing 10 % CWP than 20 % CWP, which again indicates the existence of excessive number of CWP particles can reduce concrete thermal stability.

Fig. 12 summarizes the mass loss (%) due to dehydration (Ldh), dehydroxylation (Ldx) and decarbonation (Ldc) calculated based on the temperature ranges suggested by Bhatty [69], Pane and Hansen [70] and Monteagudo, Moragues, Gálvez, Casati and Reyes [71]. The results indicate that mass loss due to Ldh increases with CWP increment. At CWP of 20 %, the mass loss due to Ldh is 1.15, 1.17, and 1.16 times larger than the concrete sample without CWP based on Bhatty [69], Pane and Hansen [70] and Monteagudo, Moragues, Gálvez, Casati and Reyes [71], respectively. The larger mass loss is likely because of the increase in C-S-H gels within the CWP content increment. The large mass loss can also be related to the formation of other hydrates, such as Gehlenite [$Ca_2Al(AlSi)O_7$], due to the existence of CWP.

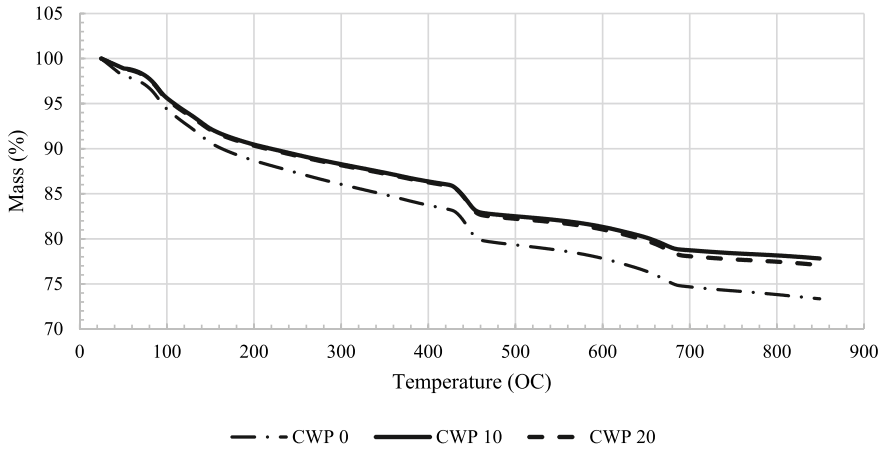

Fig. 11. TGA of concrete containing different CWP contents.

Table 9
Temperature range for dehydration (Ldh), dehydroxylation (Ldx), and decarbonation (Ldc) in different literature.

Region	Temperature ^{o}C		
	Bhatty [69]	Pane and Hansen [70]	Monteagudo, Moragues, Gálvez, Casati and Reyes [71]
Loss of the water	25.0–105	25.0–140	25.0–105
Dehydration (Ldh)	105–400	140–440	105–430
Dehydroxylation (Ldx)	400–580	440–520	430–530
Decarbonation (Ldc)	>580	>520	>530

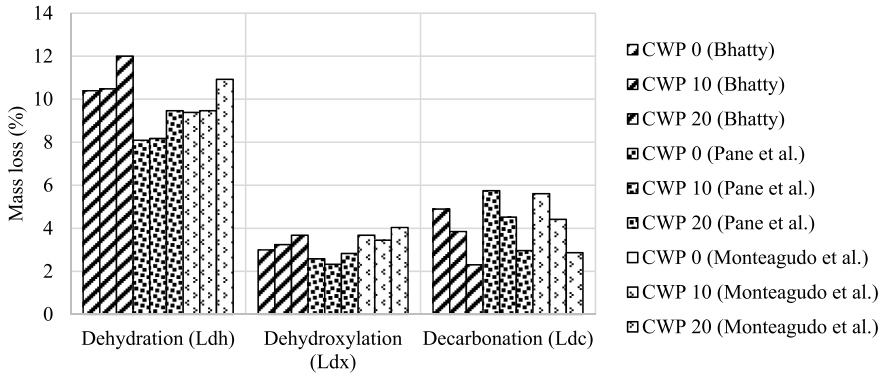

Fig. 12. TGA of concrete containing different CWP contents.

It is generally believed that an increase in pozzolanic reaction consumes more Portlandite, and thus, the mass loss due to Ldx for concrete with CWP should be less than that for concrete without CWP. However, Fig. 12 does not support this finding. The extent of Ldx determined for concrete containing 20 % CWP is higher than concrete without CWP using temperature range suggested by Bhatty [69], Pane and Hansen [70] and Monteagudo, Moragues, Gálvez, Casati and Reyes [71]. This may be because adding CWP can reduce the concrete porosity and size of defects/cracks within concrete. As a result, more water is trapped inside the concrete mix, contributing to cement hydration and the formation of the Portlandite. Although a large amount of Portlandite can be consumed by pozzolanic reaction, the composition is still more than that of concrete without CWP. Fig. 12 also shows that the mass loss due to Ldc reduces as CWP content increases in concrete. This is also because the more CWP content in the mix resulted in lower porosity; thus, CO_2 could not diffuse more easily than in concrete mixes, which can hinder the decomposition of Calcite.

Table 10 compares the Ldh, Ldx, and Ldc of concrete containing various SCMs (using the method suggested by Pane and Hansen [70]. Table 10 also shows that the mass loss due to Ldh is 9.5 % for concrete containing 20 % CWP. For concrete containing 15 % SF, the mass loss due to Ldh has already reached 10 %. SF contains more SiO_2 (over 90 %) than CWP, leading to a higher pozzolanic reaction at the same cement replacement level.

Other factors, such as water-cement ratio and cement types, can also affect mass loss. However, the general trend summarized in Table 10 suggests that the mass loss due to Ldh for CWP concrete is significantly larger than that of FA and slag concrete at the same

Table 10
Comparison of Ldh, Ldx, Ldc of concrete containing different SCMs.

	w/c	Replacement material	Replacement level (%)	Ldh (%)	Ldx (%)	Ldc (%)
This study	0.45	CWP	10	8.2	2.3	4.5
	0.48		20	9.5	2.8	2.9
Narattha, Thongsanitgarn and Chaipanich [56]	0.48	FA (Class F)	15	7.4	4.6	4.0
Lekhya and Kumar [35]	0.28	SF + FA (Class F)	15(SF)+10(FA)	4.5	2.5	4.5
	0.28	SF + FA (Class F)	15(SF)+15(FA)	3.6	1.2	4.8
Esteves [72]	–	SF	15	10.0	1.0	2.5
Teixeira, Camões, Branco, Aguiar and Fangueiro [73]	0.50	FA (Class F)[a]	50	6.5	1.0	3.5
Chaipanich, Thongsomboon and Chomyen [74]	0.49	FA (Class F)[a]	50	5.5	2.5	9.0
Ho, Doh, Chin and Li [75]	0.35	Fine steel slag	10	2.0	0.7	5.3
	0.35	Coarse steel slag	10	4.4	2.1	8.0
Mendes, Sanjayan and Collins [76]	0.50	Slag (BFS)	35	6.0	4.1	3.0
			50	9.2	3.1	2.1
			65	9.3	2.3	1.5

[a] [2]Very limited studies are on Class C FA, and thus only Class F FA is summarized in the table.

cement replacement ratio. The mass loss due to Ldh for concrete, when 10 % CWP replaces concrete, is 4.10 and 2.15 times larger than that of the concrete containing 10 % fine and coarse steel slag and 1.25–1.48 times larger than that of the concrete containing over 50 % of FA (Class F). Table 10 further indicates that the level of pozzolanic reaction is less significant for FA and slag concrete than CWP concrete.

Table 10 also shows that the mass loss due to Ldx (%) for CWP concrete is larger than that of SF, FA and slag concrete at similar cement replacement levels, but the reason can be different. For SF concrete, the level of pozzolanic reaction is higher than CWP concrete, which consumes more Portlandite. For FA and slag concrete, adding FA and slag can increase the concrete porosity and reduce the amount of water that is trapped within the concrete to form Portlandite. In summary, CWP concrete has more Portlandite than concrete with other SCMS, which can increase its potential to convert to Calcite in the concrete mix and seal microcracks within the concrete and increase its thermal insulation.

The degree of hydration can also be quantified through TGA results as suggested by Bhatty [69], following the equation below:

$$W_B = Ldh + Ldx + 0.41(Ldc) \tag{5}$$

$$\alpha = \frac{W_B}{0.24} \tag{6}$$

where W_B is the chemically bound water and α is the degree of hydration. The results are shown in Fig. 13. It can be seen from Fig. 13 that the degree of hydration increases by 1.1 times when the CWP replacement ratio increases to 20 % in concrete due to the pozzolanic reaction and formation of other hydrates. The TGA, thus, shows the quantitative evidence that the existence of CWP can contribute to pozzolanic reaction, leading to faster strength development and better thermal insulation.

3.6. XRD analysis

Fig. 14 shows the diffractograms of concrete sample containing different levels of CWP. The presences of different phases, such as, Ettringite, Portlandite, Calcite, C-S-H, and Gehlenite are also displayed in Fig. 14. The analysis failed to identify the C-A-H phase in the concrete mix, and this is likely because C-A-H is not stable and can react with calcium sulphate to form Ettringite within the concrete mix [77]. The analysis also did not find the presence of ASR reaction products, indicating that the level of ASR reaction is not evident within these mixes.

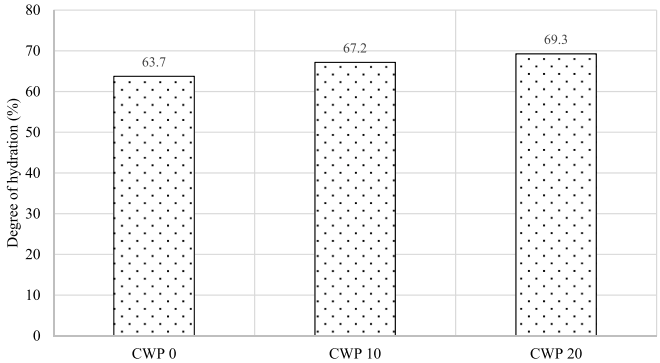

Fig. 13. Degree of cement hydration in concrete samples with varying CWP contents.

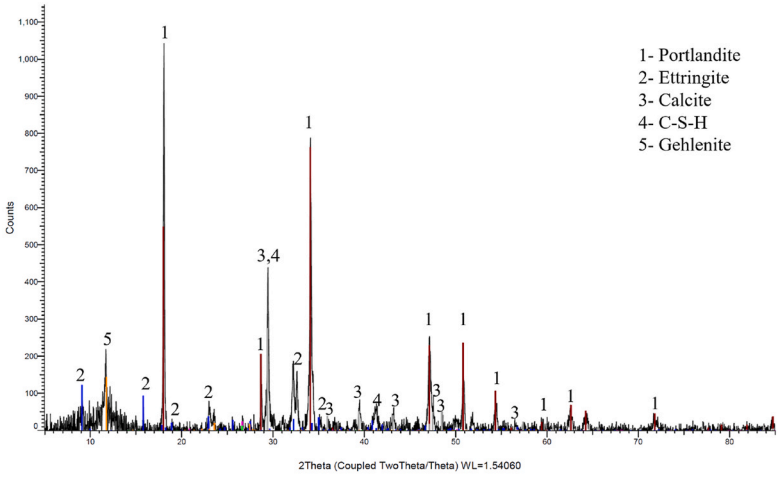

(a) CWP 0%

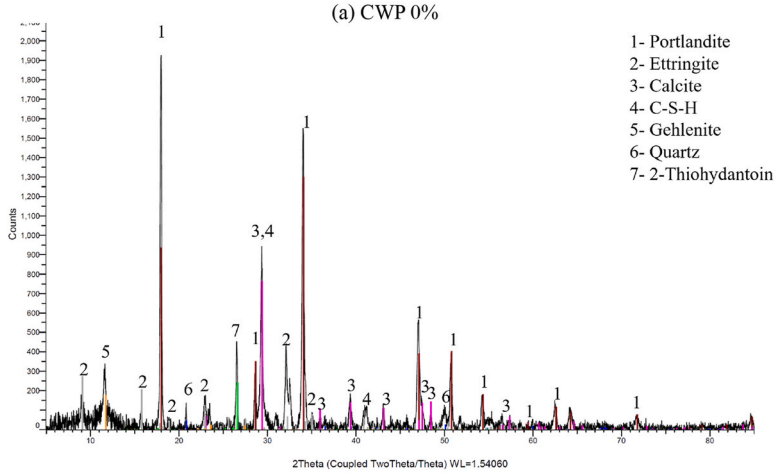

(b) CWP 10%

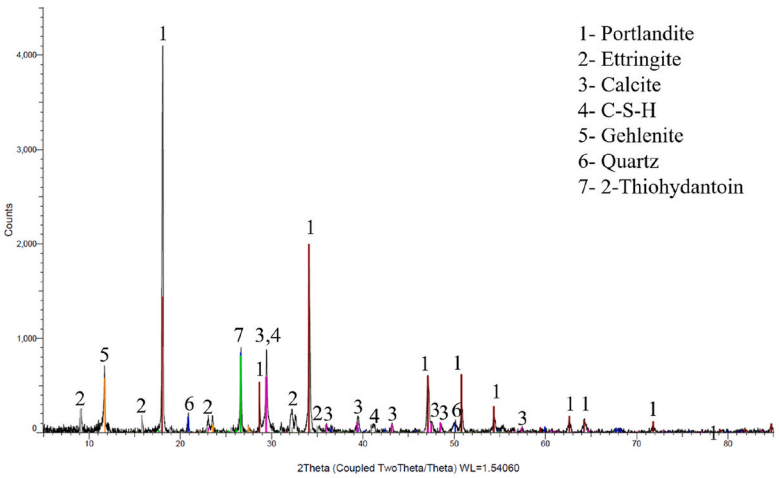

(c) CWP 20%

Fig. 14. XRD diffractograms of concrete samples containing different contents of CWP.

The XRD analysis shows an increasing peak density for C-S-H and Ettringite with increasing CWP replacement rate, indicating that adding CWP can contribute to pozzolanic reaction. There is also an increase in the peak density of Portlandite when CWP content increases. The results are in accordance with those from TGA. In addition, Fig. 14 confirms that adding CWP can increase the formation of Gehlenite due to the increase in SiO_2, Al_2O_3 and CaO in concrete mixes. A small increment in the amount of Genlenite in concrete can contribute to the thermal stability of concrete and increase its thermal insulation [78]. However, too much Genlenite can affect the cement hydration. This can explain why the 28-day compressive strength for concrete containing 20 % of CWP is lower than that containing 10 % of CWP, as shown in Fig. 6a.

4. Discussion

The current investigation found that although adding CWP can improve the thermal insulation of concrete, the strength and thermal stability of concrete containing 10 % CWP is better than that of concrete containing 20 % CWP. Li, Joseph, Zhang and Zhang [3] have estimated the fire performance of CWP concrete through Cone calorimeter tests and have similar findings: replacing cement with 10 % CWP can improve the fire performance of concrete (e.g., less mass loss and strength reduction over CWP concrete samples after fire exposure), but adding 20 % CWP can reduce these improvements. Also, Li, Joseph, Zhang and Zhang [3] indicated that the fire performance of 20 % is worse than that of concrete without CWP, despite the former having less porosity and mass decomposition after heating through porosity analysis and TGA as presented in this study. This may be because water is trapped in the pores of concrete containing 20 %, and during the fire, the entrapped water vaporizes during and can build up pressure. The relatively small pore size can increase the built-up pressure and thus deteriorate the fire resistance by forming cracks and make the sample prone to spalling. Further investigations are needed to study the performance of CWP concrete exposed to fire, such as, performing detailed SEM analysis on concrete samples exposed to elevated temperatures to investigate the formation of cracks.

Results collected in Section 3 support the findings that the reduction in concrete porosity can reduce the thermal conductivity of concrete. As explained, the void-filling impact of CWP can convert big voids/defects in concrete into a few smaller ones and increase the thickness of shells surrounding voids that protect the cement paste. It is worth noting that studies still show conflicting findings. For example, Narayanan and Ramamurthy [79] indicated that an increase in concrete porosity can reduce the concrete porosity as it can enhance the amount of air inside the cement matrix of the concrete, and the air has lower thermal conductivity than concrete mixtures. Concrete thermal conductivity can not only be affected by porosity but also by the pore structure (open or closed pores), the volume of water-entrapped holes and the size of pores in concrete [53]. The concrete mix, including the cement and aggregate type, the water-cement ratio, and superplasticizers, can also affect the formation and growth of the shells surrounding concrete voids. Thus, further studies are needed to investigate the effect of pore structure, pore infill and the pore size on concrete thermal conductivity for concrete containing CWP and other SCMs. High-resolution micro-CT coupled with 3D image analysis and X-ray Computed Tomography (XCT) can be used for these studies.

It can be found that pozzolanic reaction and the formation of the C-S-H gels are one of the major reasons that affect the concrete macro-properties (such as strength development and thermal insulation) and micro-properties (such as porosity and the phase in concrete). C-S-H has various morphologies that can be related to the element composition of SCMs, the concrete mix design, curing time, and the temperature of concrete manufacturing. It has been found that C-S-H gels can contribute more to the concrete strength, durability, and thermal insulation if it has a cubic/rhombohedral morphology than irregular shapes [80]. It is important to investigate the effect of CWS content, concrete mix types, water-cement ratio, curing time, and manufacturing temperature on the morphology of C-S-H gels to optimize the CWP manufacturing procedure to maximize the number of C-S-H gels with cubic/rhombohedral morphology. This can be done by performing SEM, XRD, and transmission electron microscopy (TEM) on CWP concrete samples under different manufacturing conditions.

The paper indicated a low level of ASR reaction for concrete with and without CWP. However, ASR reaction can be affected by concrete aging and the exposure environment (e.g., alkaline environment, such as a marine environment, can contribute to ASR reaction) [81]. This is especially the concern for concrete containing more than 20 % of CWP, as there is a possibility of a reduction in bonding strength due to excessive CWP particles. Further studies are needed to quantify the level of ASR reaction for CWP concrete at different aging conditions and exposed to various environments.

5. Main conclusions

This paper presents a comprehensive experimental investigation into the changes in macro-properties (*i.e.,* strength development during curing and thermal conductivity at elevated temperatures) and micro-properties (porosity, the level of pozzolanic and ASR reaction, cement hydration degree) of concrete when ceramic waste powder (CWP) is used as a partial cement replacement. The following are some major findings.

- Replacing cement with 10 % or 20 % CWP enhances early-age strength development and thermal insulation at room and elevated temperatures. This is because adding CWP can reduce concrete porosity through the void-filling effect and improve pozzolanic activity, leading to more stable microstructures by enhancing bonding between hydration products, aggregate particles, and unhydrated cement grains. As a result, fewer pores and cracks have been observed at the ITZ in BSE-SEM analyses.
- A strong, positive correlation has been found between the SiO_2 concentration of SCMs and the 28-day strength of concrete, as an increase in SiO_2 concentration can enhance pozzolanic reaction. This correlation analysis further confirms that an improved pozzolanic reaction is a key factor in the strength development of CWP concrete.

- The BSE-SEM analyses showed around 60 % reduction in porosity at the interfacial transition zone in CWP concrete, while TGA results showed around 9 % increase in cement hydration when 20 % of cement is replaced with CWP. Both changes occur because adding CWP can lead to void filling and enhance pozzolanic activity. Further, TGA and XRD results indicated an increase in C-S-H gel formation (pozzolanic activity products).
- A 10 % CWP replacement is identified as the optimal ratio for balancing strength, durability, and thermal performance, whereas concrete with 20 % CWP may show reduced strength and thermal stability. This is because adding too much CWP can affect the bonding between cement and aggregate.
- Compared to fly ash and slag, CWP concrete shows more notable improvements in strength, porosity reduction, and pozzolanic reaction due to its fine size and high SiO2 content.

CRediT authorship contribution statement

Le Li: Writing – review & editing, Writing – original draft, Methodology, Investigation, Conceptualization. **Boran Zhang:** Resources, Methodology, Investigation. **Paul Joseph:** Writing – review & editing, Methodology. **Xuelin Zhang:** Investigation. **Lihai Zhang:** Writing – review & editing, Supervision, Methodology, Conceptualization.

Data statement

The data that support the findings of this study are available on request from the corresponding author.

Declaration of generative AI and AI-assisted technologies in the manuscript preparation process

During the preparation of this work the authors used Grammarly in order to review the writing. After using this tool/service, the authors reviewed and edited the content as needed and take full responsibility for the content of the published article.

Declaration of competing interest

The authors declare that they have no known competing financial interests or personal relationships that could have appeared to influence the work reported in this paper.

Acknowledgement

Thanks to Southern Cross Ceramics for their valuable help and support in the study, including providing ceramic waste powder and finalizing the test plan.

Data availability

Data will be made available on request.

References

[1] S. Saint Akadiri, A.A. Alola, G. Olasehinde-Williams, M.U. Etokakpan, The role of electricity consumption, globalization and economic growth in carbon dioxide emissions and its implications for environmental sustainability targets, Sci. Total Environ. 708 (2020) 134653.
[2] L. Barcelo, J. Kline, G. Walenta, E. Gartner, Cement and carbon emissions, Mater. Struct. 47 (2014) 1055–1065.
[3] L. Li, P. Joseph, X. Zhang, L. Zhang, A study of some relevant properties of concrete incorporating waste ceramic powder as a cement replacement agent, J. Build. Eng. 87 (2024) 109106.
[4] M. Bhargav, R. Kansal, Experimental investigation to substitute of cement with ceramic tiles powder in concrete, Int. J. Res. Appl. Sci. Eng. Technol. 8 (2020) 302–307.
[5] L. Gautam, P. Kalla, J.K. Jain, R. Choudhary, A. Jain, Robustness of self-compacting concrete incorporating bone China ceramic waste powder along with granite cutting waste for sustainable development, J. Clean. Prod. 367 (2022) 132969.
[6] A.K. Parashar, P. Sharma, N. Sharma, An investigation on properties of concrete with the adding of waste of ceramic and micro silica, Mater. Today Proc. 62 (2022) 4036–4040.
[7] D.M. Kannan, S.H. Aboubakr, A.S. El-Dieb, M.M.R. Taha, High performance concrete incorporating ceramic waste powder as large partial replacement of Portland cement, Constr. Build. Mater. 144 (2017) 35–41.
[8] A.D. Raval, D.I.N. Patel, J. Pitroda, Ceramic waste: effective replacement of cement for establishing sustainable concrete, Int. J. Eng. Trends Technol. 4 (2013) 2324–2329.
[9] H. Patel, N. Arora, S.R. Vaniya, Use of Ceramic Waste Powder in Cement Concrete, vol. 2, International Journal for Innovative Research in Science & Technology, 2015, pp. 91–97.
[10] IS456, Plain and Reinforced concrete-code of Practice, Bureau of Indian Standards, New Delhi, 2000.
[11] A. Richardson, Strength development of plain concrete compared to concrete with a non-chloride accelerating admixture, Struct. Surv. 25 (2007) 418–423.
[12] M.J. Taher, E. Abed, M.S. Hashim, Using ceramic waste tile powder as a sustainable and eco-friendly partial cement replacement in concrete production, Mater. Today Proc. (2023).
[13] X. Chen, D. Zhang, S. Cheng, X. Xu, C. Zhao, X. Wang, Q. Wu, X. Bai, Sustainable reuse of ceramic waste powder as a supplementary cementitious material in recycled aggregate concrete: mechanical properties, durability and microstructure assessment, J. Build. Eng. 52 (2022) 104418.
[14] A.S. El-Dieb, M.R. Taha, S.I. Abu-Eishah, The Use of Ceramic Waste Powder (CWP) in Making eco-friendly Concretes, Ceramic materials-synthesis, Characterization, Applications and Recycling, IntechOpen, 2018.

[15] P. Awoyera, J. Akinmusuru, A. Dawson, J. Ndambuki, N. Thom, Microstructural characteristics, porosity and strength development in ceramic-laterized concrete, Cement Concr. Compos. 86 (2018) 224–237.
[16] Q. Chen, J. Zhang, Z. Wang, T. Zhao, Z. Wang, A review of the interfacial transition zones in concrete: identification, physical characteristics, and mechanical properties, Eng. Fract. Mech. (2024) 109979.
[17] L. Li, W. Liu, Q. You, M. Chen, Q. Zeng, Waste ceramic powder as a pozzolanic supplementary filler of cement for developing sustainable building materials, J. Clean. Prod. 259 (2020) 120853.
[18] M. Mohit, H. Haftbaradaran, H.T. Riahi, Investigating the ternary cement containing Portland cement, ceramic waste powder, and limestone, Constr. Build. Mater. 369 (2023) 130596.
[19] Y. Tan, K. Tang, Evaluate the effect of coarse aggregates on cement hydration heat and concrete temperature modelling using isothermal calorimetry, Heliyon 10 (2024) e38322.
[20] R. Demirboğa, Thermal conductivity and compressive strength of concrete incorporation with mineral admixtures, Build. Environ. 42 (2007) 2467–2471.
[21] Y. Liu, X. Zhou, C. Lv, Y. Yang, T. Liu, Use of silica fume and GGBS to improve frost resistance of ECC with high-volume fly ash, Adv. Civ. Eng. 2018 (2018) 7987589.
[22] B. Alabadan, C. Njoku, M. Yusuf, The potentials of groundnut shell ash as concrete admixture, Agric. Eng. Int. CIGR J. (2006).
[23] P.T. Cherop, S.L. Kiambi, E.K. Kosgey, Effect of non-ionic cellulose ethers on properties of white Portland cement, Int. J. Appl. Eng. Res. 12 (2017) 2502–2508.
[24] AS1012.2, Methods of Testing Concrete, Method 2: Preparing Concrete Mixes in the Laboratory, Standards Australia, Sydney, 2014.
[25] AS1012.9, Methods of Testing Concrete Compressive Strength Tests - Concrete, Mortar and Grout Specimens, Standards Australia, Sydney, 2014.
[26] ISO22007-2, Plastics — Determination of Thermal Conductivity and Thermal Diffusivity, Part 2: Transient Plane Heat Source (Hot Disc) Method, International Organization for Standardization, Switzerland, 2022.
[27] A. Ergün, G. Kürklü, B.M. Serhat, M.Y. Mansour, The effect of cement dosage on mechanical properties of concrete exposed to high temperatures, Fire Saf. J. 55 (2013) 160–167.
[28] ASTMC1723-16, Standard Guide for Examination of Hardened Concrete Using Scanning Electron Microscopy, ASTM International, West Conshohocken, Pennsylvania, United States, 2012, p. 9.
[29] R.S. Edwin, M. Mushthofa, E. Gruyaert, N. De Belie, Quantitative analysis on porosity of reactive powder concrete based on automated analysis of back-scattered-electron images, Cement Concr. Compos. 96 (2019) 1–10.
[30] Y. Song, G. Dai, J. Zhou, Z. Bian, L. Zhao, L. Song, Characterizing porous volume of cement-based concrete by multiscale image analysis, J. Mater. Civ. Eng. 32 (2020) 04020267.
[31] Y. Song, J.-w. Zhou, Z.-n. Bian, G.-z. Dai, Pore structure characterization of hardened cement paste by multiple methods, Adv. Mater. Sci. Eng. 2019 (2019) 3726953.
[32] J. Zheng, Y. Gao, H. Zhang, Y. Lei, J. Zhang, OTSU multi-threshold image segmentation based on improved particle swarm algorithm, Appl. Sci. 12 (2022) 11514.
[33] H. Wong, N. Buenfeld, M. Head, Estimating transport properties of mortars using image analysis on backscattered electron images, Cement Concr. Res. 36 (2006) 1556–1566.
[34] K.A. Ahmad, N. Abdul Hassan, M.E. Abdullah, M.A. Bilema, N. Usman, A.A.M. Al Allam, M.R.B. Hainin, Image processing procedure to quantify the internal structure of porous asphalt concrete, Multidiscip. Model. Mater. Struct. 15 (2019) 206–226.
[35] A. Lekhya, N.S. Kumar, A study on the effective utilization of ultrafine fly ash and silica fume content in high-performance concrete through an experimental approach, Heliyon 10 (2024) e39678.
[36] V. Kanchanason, J. Plank, Effect of calcium silicate hydrate–polycarboxylate ether (CSH–PCE) nanocomposite as accelerating admixture on early strength enhancement of slag and calcined clay blended cements, Cement Concr. Res. 119 (2019) 44–50.
[37] M.M.A. Elahi, C.R. Shearer, A.N.R. Reza, A.K. Saha, M.N.N. Khan, M.M. Hossain, P.K. Sarker, Improving the sulfate attack resistance of concrete by using supplementary cementitious materials (SCMs): a review, Constr. Build. Mater. 281 (2021) 122628.
[38] ACI-CODE-318-19(22), Building Code Requirements for Structural Concrete and Commentary (Reapproved 2022), American Concrete Institute, Farmington Hills, Michigan, 2019, p. 624.
[39] S. Popovics, J. Ujhelyi, Contribution to the concrete strength versus water-cement ratio relationship, J. Mater. Civ. Eng. 20 (2008) 459–463.
[40] K.A. Knight, P.R. Cunningham, S.A. Miller, Optimizing supplementary cementitious material replacement to minimize the environmental impacts of concrete, Cement Concr. Compos. 139 (2023) 105049.
[41] M. Mazloom, A. Ramezanianpour, J. Brooks, Effect of silica fume on mechanical properties of high-strength concrete, Cement Concr. Compos. 26 (2004) 347–357.
[42] H. Wong, H.A. Razak, Efficiency of calcined kaolin and silica fume as cement replacement material for strength performance, Cement Concr. Res. 35 (2005) 696–702.
[43] A. Behnood, H. Ziari, Effects of silica fume addition and water to cement ratio on the properties of high-strength concrete after exposure to high temperatures, Cement Concr. Compos. 30 (2008) 106–112.
[44] A. Saha, S. Pan, S. Pan, Strength development characteristics of high strength concrete incorporating an Indian fly ash, Int. J. Sci. Technol. 2 (2014) 101–107.
[45] P. Chindaprasirt, S. Rukzon, Strength, porosity and corrosion resistance of ternary blend Portland cement, rice husk ash and fly ash mortar, Constr. Build. Mater. 22 (2008) 1601–1606.
[46] A. Oner, S. Akyuz, An experimental study on optimum usage of GGBS for the compressive strength of concrete, Cement Concr. Compos. 29 (2007) 505–514.
[47] A.G. Asuero, A. Sayago, A. González, The correlation coefficient: an overview, Crit. Rev. Anal. Chem. 36 (2006) 41–59.
[48] H.F. Taylor, Cement Chemistry, Thomas Telford, London, 1997.
[49] A. Moshiri, A. Morshedifard, D. Stefaniuk, S. El Awad, T. Phatak, K.J. Krzywiński, D.F. Rodrigues, M.J.A. Qomi, K.J. Krakowiak, Organic cross-linking decreases the thermal conductivity of calcium silicate hydrates, Cement Concr. Res. 174 (2023) 107324.
[50] H.A. Shah, Q. Yuan, S. Zuo, Air Entrainment in Fresh Concrete and its Effects on Hardened concrete-a, 2020.
[51] M.T. Lakhiar, S.Y. Kong, Y. Bai, S. Susilawati, I. Zahidi, S.C. Paul, M.E. Raghunandan, Thermal and mechanical properties of concrete incorporating silica fume and waste rubber powder, Polymers 14 (2022) 4858.
[52] Z.N. Lallas, M.J. Gombeda, F. Mendonca, Review of supplementary cementitious materials with implications for age-dependent concrete properties affecting precast concrete, PCI J. 68 (2023).
[53] J. Xiao, Z. Lv, Z. Duan, C. Zhang, Pore structure characteristics, modulation and its effect on concrete properties: a review, Constr. Build. Mater. 397 (2023) 132430.
[54] Y. Du, Y. Ge, Multiphase model for predicting the thermal conductivity of cement paste and its applications, Materials 14 (2021) 4525.
[55] D. Mostofinejad, O. Aghamohammadi, H. Bahmani, S. Ebrahimi, Improving thermal characteristics and energy absorption of concrete by recycled rubber and silica fume, Developments in the Built Environment 16 (2023) 100221.
[56] C. Narattha, P. Thongsanitgarn, A. Chaipanich, Thermogravimetry analysis, compressive strength and thermal conductivity tests of non-autoclaved aerated Portland cement–fly ash–silica fume concrete, J. Therm. Anal. Calorim. 122 (2015) 11–20.
[57] Z. Zhao, X. Qu, F. Li, J. Wei, Effects of steel slag and silica fume additions on compressive strength and thermal properties of lime-fly ash pastes, Constr. Build. Mater. 183 (2018) 439–450.
[58] K.-H. Kim, S.-E. Jeon, J.-K. Kim, S. Yang, An experimental study on thermal conductivity of concrete, Cement Concr. Res. 33 (2003) 363–371.
[59] R. Demirboğa, R. Gül, The effects of expanded perlite aggregate, silica fume and fly ash on the thermal conductivity of lightweight concrete, Cement Concr. Res. 33 (2003) 723–727.
[60] M.J. Chinchillas-Chinchillas, C.A. Rosas-Casarez, S.P. Arredondo-Rea, J.M. Gómez-Soberón, R. Corral-Higuera, SEM image analysis in permeable recycled concretes with silica fume. A quantitative comparison of porosity and the ITZ, Materials 12 (2019) 2201.

[61] C.-S. Poon, S. Kou, L. Lam, Compressive strength, chloride diffusivity and pore structure of high performance metakaolin and silica fume concrete, Constr. Build. Mater. 20 (2006) 858–865.
[62] T. Luo, C. Hua, F. Liu, Q. Sun, Y. Yi, X. Pan, Effect of adding solid waste silica fume as a cement paste replacement on the properties of fresh and hardened concrete, Case Stud. Constr. Mater. 16 (2022) e01048.
[63] A.A. Gonçalves Junior, E.I. Jussiani, A.C. Andrello, R.D. Vanderlei, B.M. Toralles, Ecoefficient cementitious materials with high levels of Portland cement replacement using blast furnace slag, J. Mater. Civ. Eng. 36 (2024) 04024229.
[64] A. Attari, C. McNally, M.G. Richardson, A combined SEM–Calorimetric approach for assessing hydration and porosity development in GGBS concrete, Cement Concr. Compos. 68 (2016) 46–56.
[65] C.S. Poon, L. Lam, Y.L. Wong, Effects of fly ash and silica fume on interfacial porosity of concrete, J. Mater. Civ. Eng. 11 (1999) 197–205.
[66] J. Yang, Q. Ding, G. Zhang, D. Hou, M. Zhao, J. Cao, Effect of sulfate attack on the composition and micro-mechanical properties of CASH gel in cement-slag paste: a combined study of nanoindentation and SEM-EDS, Constr. Build. Mater. 345 (2022) 128275.
[67] R. Vigil de la Villa Mencía, M. Frías, S.M. Ramírez, L.F. Carrasco, R.G. Giménez, Concrete/glass construction and demolition waste (CDW) synergies in ternary eco-cement-paste mineralogy, Materials 15 (2022) 4661.
[68] R. Esposito, M. Hendriks, Literature review of modelling approaches for ASR in concrete: a new perspective, European Journal of Environmental and Civil Engineering 23 (2019) 1311–1331.
[69] J.I. Bhatty, Hydration versus strength in a portland cement developed from domestic mineral wastes—A comparative study, Thermochim. Acta 106 (1986) 93–103.
[70] I. Pane, W. Hansen, Investigation of blended cement hydration by isothermal calorimetry and thermal analysis, Cement Concr. Res. 35 (2005) 1155–1164.
[71] S. Monteagudo, A. Moragues, J. Gálvez, M. Casati, E. Reyes, The degree of hydration assessment of blended cement pastes by differential thermal and thermogravimetric analysis. Morphological evolution of the solid phases, Thermochim. Acta 592 (2014) 37–51.
[72] L.P. Esteves, On the hydration of water-entrained cement–silica systems: combined SEM, XRD and thermal analysis in cement pastes, Thermochim. Acta 518 (2011) 27–35.
[73] E.R. Teixeira, A. Camões, F. Branco, J. Aguiar, R. Fangueiro, Recycling of biomass and coal fly ash as cement replacement material and its effect on hydration and carbonation of concrete, Waste Manag. 94 (2019) 39–48.
[74] A. Chaipanich, S. Thongsomboon, P. Chomyen, Thermogravimetric analysis and phase characterizations of Portland fly ash limestone cements, J. Therm. Anal. Calorim. 142 (2020) 183–190.
[75] C.M. Ho, S.I. Doh, S.C. Chin, X. Li, The effect of particle sizes of steel slag as cement replacement in high strength concrete under elevated temperatures, Constr. Build. Mater. 411 (2024) 134531.
[76] A. Mendes, J. Sanjayan, F. Collins, Phase transformations and mechanical strength of OPC/Slag pastes submitted to high temperatures, Mater. Struct. 41 (2008) 345–350.
[77] A. Quennoz, K.L. Scrivener, Interactions between alite and C3A-gypsum hydrations in model cements, Cement Concr. Res. 44 (2013) 46–54.
[78] O. Gencel, O.Y. Bayraktar, G. Kaplan, O. Arslan, M. Nodehi, A. Benli, A. Gholampour, T. Ozbakkaloglu, Lightweight foam concrete containing expanded perlite and glass sand: Physico-mechanical, durability, and insulation properties, Constr. Build. Mater. 320 (2022) 126187.
[79] N. Narayanan, K. Ramamurthy, Structure and properties of aerated concrete: a review, Cement Concr. Compos. 22 (2000) 321–329.
[80] R. Shahsavari, S.H. Hwang, Morphogenesis of cement hydrate: from natural CSH to synthetic CSH, Cement based materials (2018) 79–90.
[81] B. Fournier, J.H. Ideker, K.J. Folliard, M.D. Thomas, P.-C. Nkinamubanzi, R. Chevrier, Effect of environmental conditions on expansion in concrete due to alkali–silica reaction (ASR), Mater. Char. 60 (2009) 669–679.